Fabrication and Characterization of MnS Thick Films by Screen Printing Technique

Chetan R. Yewale[1], Rajendra V. Wagh[2], Vaishali T. Salunke[3], Arun V. Patil[4], Satish S. Mandawade[5]

[1,4]Department of Physics and Research Centre, MGV's MSG Arts, Science and Commerce College, Malegaon, Dist: Nashik, Maharashtra, India
[2]MVP's Arts, Commerce and Science College, Nandgaon, At-Post- Nandgaon Dist: Nashik, Maharashtra, India
[3]Department of Electronic Science, MGV's MSG Arts, Science and Commerce College, Malegaon, Dist: Nashik, Maharashtra, India
[4]Department of Physics, MGV's, Arts, Science and Commerce College, Nimgaon, Dist. Nashik, Maharashtra, India
[5]Department of Physics and Research Centre, MGV's MSG Arts, Science and Commerce College, Malegaon, Dist. Nashik, Affiliated to Savitribai Phule Pune University, Maharashtra, India

Abstract:
In the present work, MnS thick films were fabricated on glass substrates using commercially available analytical reagent (AR) grade MnS nanopowder and the screen-printing technique. A homogeneous screen-printing paste was prepared by mixing MnS nanopowder with BCA and ethyl cellulose, in a 70:30 weight ratio. The printed films were dried under an infrared (IR) lamp for 30 min and subsequently annealed in a closed muffle furnace at 200 °C for 2 h. The structural, morphological and elemental characteristics of the prepared MnS thick films were investigated using X-ray diffraction (XRD), scanning electron microscopy (SEM), and energy-dispersive X-ray spectroscopy (EDX). XRD analysis confirmed the formation of the hexagonal wurtzite γ-MnS phase, with the diffraction pattern indexed according to JCPDS Card No. 40-1289. The average crystallite size of the MnS thick film was determined to be 86 nm using the Debye–Scherrer equation. SEM analysis revealed a continuous and fine-grained surface morphology with localized particle agglomeration and irregular surface cavities. EDX analysis confirmed the presence of Mn and S as the principal constituent elements, with measured concentrations of 63.75 wt. % Mn and 36.25 wt. % S. The results demonstrate that the screen-printing technique provides an effective route for the fabrication of structurally stable MnS thick films with well-defined elemental composition and characteristic surface morphology.

Keywords: Thick films, structural, morphological, XRD analysis, particle agglomeration.

1. Introduction

The development of functional semiconductor materials with controlled structural and morphological characteristics has received considerable attention because the physical properties of a material are strongly influenced by its crystal structure, grain morphology, composition and microstructural features. Semiconductor films in particular provide an effective platform for integrating functional materials onto substrates and have been investigated extensively for electronic, sensing, optoelectronic, photovoltaic and energy-related applications. Within this broad class of materials, transition-metal sulfides have attracted

significant interest because of their diverse crystal structures, tunable electronic properties, chemical stability and distinctive interactions between metal cations and sulfur anions. Recent reviews have emphasized that transition-metal sulfides possess composition-dependent structural and electronic characteristics and offer considerable scope for functional materials development (Ali et al., 2025).

Manganese sulfide (MnS) is an important transition-metal chalcogenide consisting of manganese and sulfur and belongs to a technologically relevant class of semiconducting sulfide materials. MnS has attracted scientific interest because of its semiconducting, magnetic and structural characteristics. The material exhibits different polymorphic forms, and its structural phase is strongly associated with the conditions employed during synthesis and film growth. Reported MnS phases include cubic α-MnS, cubic β-MnS and hexagonal γ-MnS, with the formation and stability of these phases depending on deposition conditions, precursor chemistry, temperature and post-deposition treatment. The coexistence of multiple structural forms makes MnS particularly interesting for systematic investigation of the relationship between preparation conditions and material properties (Gowthami et al., 2017). The crystal structure of MnS plays a central role in determining its physical properties. α-MnS possesses a cubic rock-salt structure, whereas β-MnS exhibits a zinc-blende-type cubic structure and γ-MnS crystallizes in a hexagonal wurtzite structure. Experimental investigations have demonstrated that different preparation techniques produce different MnS phases. For example, chemical bath deposition has produced hexagonal γ-MnS with preferential orientation along the (002) plane, while other synthesis approaches have produced cubic α-MnS. Such structural variations directly influence crystallinity, lattice parameters, crystallite dimensions, grain growth and surface morphology (Gowthami et al., 2017; Ghosh et al., 2021). Therefore, identification of the crystalline phase represents a fundamental step in establishing the structure–property relationship of MnS-based films. MnS has also been investigated as a semiconductor for several functional applications. Earlier studies identified MnS as a wide-band-gap semiconductor with reported band-gap values depending on the crystal phase, deposition conditions and film characteristics. Its combination of semiconductor behavior and manganese-related magnetic properties has generated interest in optoelectronic and multifunctional material systems. Recent investigations continue to examine MnS films for applications associated with sensors, photoconductive devices, solar-cell structures, supercapacitors and related electronic systems (Jadhav et al., 2025). The broad functional potential of MnS originates from its chemical composition and structural flexibility, while its performance in a particular application depends strongly on crystallinity, grain structure, surface characteristics and elemental stoichiometry.

The preparation technique is therefore an important consideration in the development of MnS films. Various methods have been reported for depositing MnS, including chemical bath deposition, thermal evaporation, successive ionic layer adsorption and reaction, spray-based methods, doctor-blade deposition and other solution- and vacuum-based techniques. Chemical bath deposition has been widely employed because it provides a relatively simple route for producing MnS films under controlled solution conditions. Thermal evaporation has also been used to investigate the influence of substrate temperature and precursor quantity on film structure and morphology. Kaur et al. (2016) investigated α-MnS films prepared by thermal vacuum evaporation and demonstrated the dependence of the structural and morphological characteristics on deposition conditions. Similarly, Ghosh et al. (2021) demonstrated the preparation of α-MnS nanocrystals and films using different synthetic routes and reported cubic MnS formation in films prepared through a doctor-blade route.

For thick-film development, the screen-printing technique provides an attractive fabrication route because it enables deposition of a controlled layer of functional material over a defined substrate area. Screen printing

involves forcing a prepared material paste through a patterned screen onto a substrate, followed by drying and thermal treatment. The technique is particularly suitable for thick-film fabrication because the deposited layer contains a comparatively high loading of functional material and the process supports reproducible film formation over relatively large areas. Screen printing has been successfully employed for semiconductor oxide thick films, where subsequent thermal treatment produces mechanically stable and structurally developed functional layers. Zargar et al. (2016), for instance, reported nanocrystalline CdO thick films fabricated by screen printing and demonstrated that the resulting films possessed a polycrystalline granular structure as revealed by XRD and SEM analyses. Recent work on screen-printed V_2O_5 thick films has further demonstrated the influence of thermal treatment on crystallinity and grain development, confirming the usefulness of screen printing for producing functional thick-film materials (2026).

Despite the extensive investigation of MnS thin films using chemical bath deposition, thermal evaporation, SILAR and other deposition methods, comparatively less attention has been directed toward the fabrication of MnS thick films using screen printing. This distinction is significant because the microstructure obtained through screen printing differs from that produced through thin-film deposition processes. In a screen-printed film, the particle size and distribution of the starting MnS powder, paste formulation, thickness of the printed layer, drying conditions and subsequent heat treatment collectively influence particle packing, grain connectivity, surface morphology and phase development. Consequently, investigation of screen-printed MnS thick films provides useful information regarding the formation and microstructural characteristics of MnS in a thick-film configuration.

Among the characterization techniques available for semiconductor films, X-ray diffraction (XRD) provides direct information regarding the crystallographic structure and phase composition of the prepared material. XRD analysis identifies the diffraction peaks associated with specific crystallographic planes and permits determination of the crystal structure by comparison with standard reference data. The diffraction profile also provides information about preferential orientation and crystallite size. The crystallite size is frequently estimated using the Debye–Scherrer relation from the broadening of selected diffraction peaks. In MnS films, XRD analysis is particularly important because MnS exhibits several polymorphic structures. Previous studies have demonstrated that changes in deposition conditions produce substantial differences in MnS phase formation and crystallinity. Gowthami et al. (2017) reported hexagonal MnS films with lattice parameters consistent with the γ-MnS structure, whereas other investigations have identified cubic α-MnS depending on the preparation route.

The surface morphology of a thick film provides complementary information to the structural analysis. Scanning electron microscopy (SEM) enables direct observation of the film surface at high magnification and reveals grain shape, grain distribution, particle agglomeration, surface compactness, voids and other microstructural features. These characteristics are important because the morphology reflects the processes of nucleation, particle growth, coalescence and densification occurring during film formation and thermal treatment. In MnS films, significant differences in morphology have been reported for different preparation conditions. Gowthami et al. (2017) observed spherical grains with different size distributions in chemically deposited MnS films, while other investigations reported irregular and more regularly shaped MnS nanocrystals depending on the synthesis route. Such observations establish SEM as an essential technique for evaluating the microstructural quality of MnS thick films.

Energy-dispersive X-ray spectroscopy (EDX/EDAX) provides elemental information complementary to XRD and SEM analyses. EDX detects the characteristic X-rays emitted by the constituent elements when the

specimen is irradiated by an electron beam. For MnS films, EDX analysis confirms the presence of manganese and sulfur and provides their relative elemental proportions. Elemental analysis is particularly important for evaluating the compositional integrity of the deposited film because variations in the Mn:S ratio influence the phase formation and material characteristics. Previous investigations of MnS films have confirmed manganese and sulfur as the principal constituent elements using EDX analysis. Synthesis by chemical bath deposition, for example, produced films containing Mn and S without detectable additional elemental impurities under the reported experimental conditions (Gowthami et al., 2017).

The combined use of XRD, SEM and EDX therefore provides a coherent characterization strategy for MnS thick films. XRD establishes the crystalline phase and structural characteristics, SEM reveals the surface morphology and microstructural organization, and EDX confirms the elemental composition. These three techniques provide complementary information rather than overlapping measurements. The structural information obtained from XRD is correlated with the grain morphology observed through SEM, while EDX verifies whether the observed structural phase corresponds to the expected Mn–S composition. Previous MnS film studies have successfully employed this combination of XRD, SEM and EDX to establish phase, morphology and composition, demonstrating its suitability for fundamental characterization of manganese sulfide films.

In the present investigation, MnS thick films were fabricated using the screen-printing technique and systematically characterized using XRD, SEM and EDX. The study focuses on establishing the structural phase, crystallinity and crystallite characteristics of the prepared MnS thick films through XRD analysis, examining their surface morphology and grain distribution through SEM, and determining their elemental composition through EDX analysis. The investigation is directed toward establishing the relationship between the fabrication process and the resulting structural, morphological and compositional characteristics of MnS thick films. The study provides a focused basis for understanding the suitability of screen printing for MnS thick-film fabrication and contributes to the development of MnS-based functional thick-film materials.

2. Experimental work

2.1 Fabrication of MnS thick films

MnS thick films were fabricated on clean glass substrates using commercially available analytical reagent (AR) grade MnS nanopowder as the functional material. The MnS nanopowder was thoroughly mixed with a suitable organic binder such as BCA and ethyl cellulose to prepare a homogeneous screen-printing paste (Makinen *et al.*, 2015). The MnS powder-to-organic binder ratio was maintained at 70:30 by weight, providing appropriate paste consistency for uniform deposition as shown in Figure 1.

Figure 1: Steps of fabrication of MnS thick films

The prepared paste was applied onto the glass substrate using the screen-printing technique, producing a uniform MnS thick-film layer over the defined area of the substrate Tupe et al. (2021). The printed films were initially dried under an infrared (IR) lamp for 30 min to remove the volatile components of the organic binder and improve the adhesion of the deposited layer to the glass substrate (Li *et al.*, 2022). The dried MnS films were then placed in a closed muffle furnace and annealed at 200 °C for 2 h. Thermal treatment at 200 °C promoted the removal and decomposition of residual organic constituents Tupe et al. (2020), improved particle-to-particle contact and enhanced the adhesion and structural stability of the MnS layer. The resulting MnS thick films were cooled to room temperature inside the furnace and then used for X-ray diffraction (XRD), scanning electron microscopy (SEM), and energy-dispersive X-ray spectroscopy (EDX) characterization.

3. Result and Discussion

3.1 X-ray diffraction (XRD)

Figure 2 shows the X-ray diffraction (XRD) pattern of the MnS thick film deposited on a glass substrate and annealed at 200 °C for 2 h. The structural phase of MnS was identified by comparing the diffraction pattern with the standard JCPDS Card No. 40-1289, which corresponds to the hexagonal wurtzite (γ-MnS) phase with space group $P6_3mc$.

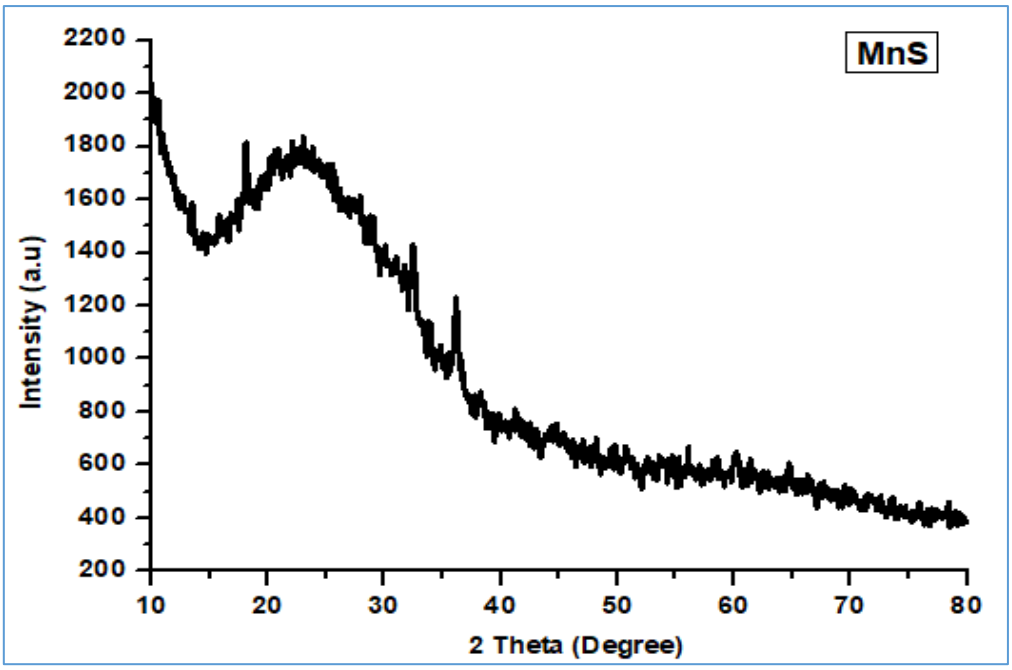

Figure 2: XRD pattern of MnS thick films

Beltran-Huarac et al. (2014) reported that γ-MnS crystallizes in the hexagonal wurtzite structure and indexed its characteristic reflections to the (100), (002), (101), (102), (110), (103), (200), (112), and (201) planes according to JCPDS Card No. 40-1289. Similarly, Dhasade et al. (2013) identified the hexagonal γ-MnS phase in MnS nanostructured films using the same JCPDS reference and assigned the observed reflections to the corresponding crystallographic planes. The characteristic diffraction positions reported for γ-MnS occur approximately at 2θ = 25.8° (100), 27.6–28.3° (002), 29.3–29.6° (101), 38.2–40.5° (102), 45.6–46.0° (110), 50.0° (103), 54.1° (112), and higher-angle reflections associated with the (200) and (201) planes.The XRD profile of the present MnS thick film exhibits a broad diffraction background with weak and poorly resolved crystalline features. This broad profile indicates relatively limited long-range structural ordering within the screen-printed MnS layer. The observed broadening is associated with the nanopowder-based film structure, particle packing and the relatively low annealing temperature of 200 °C. Hannachi et al. (2017) demonstrated that the structural characteristics of MnS films depend strongly on deposition conditions and thermal treatment, with changes in preparation parameters producing different MnS phases and variations in crystallinity and morphology. Their investigation also confirmed that MnS films exhibit either hexagonal γ-MnS or cubic β-MnS depending on the preparation conditions. Gümüş et al. (2005) reported crystalline γ-MnS films deposited on glass substrates and observed a strong reflection near 2θ = 28.26°, indexed to the (002) plane of the wurtzite MnS structure, confirming preferential growth along the c-axis. The relatively broad nature of the present diffraction profile also reflects the contribution of the amorphous glass substrate, particularly in the low-angle region. The average crystallite size of the MnS thick film was calculated to be 86 nm using the Debye–Scherrer equation by Eq. 1, based on the full width at half maximum (FWHM) of the selected diffraction peak.

$$D=K\lambda/\beta\cos\theta \qquad \text{Eq.1.}$$

Where,

D is the crystallite size, Kis the shape factor (0.9), λ is the wavelength of Cu Kα radiation (0.15406 nm), β is the FWHM of the diffraction peak in radians, and θ is the corresponding Bragg angle.

The crystallite size represents the mean dimension of coherently diffracting crystalline domains within the MnS thick film and does not necessarily correspond to the individual particle or grain size observed by SEM. This distinction is important for nanopowder-based screen-printed films, where individual particles consist of crystalline domains that undergo packing and partial coalescence during thermal treatment. Previous studies have reported substantially different crystallite sizes for MnS depending on the synthesis route and processing conditions. Beltran-Huarac et al. (2014) also confirmed the formation of highly crystalline γ-MnS with the hexagonal wurtzite structure and demonstrated the importance of crystallographic analysis in establishing the phase of MnS. Thus, the XRD analysis of the present screen-printed film establishes the hexagonal γ-MnS phase, while the broad diffraction profile and calculated 86 nm crystallite size describe the structural characteristics of the annealed MnS thick-film layer.

3.2 SEM

Figure 3(a–d) presents the SEM micrographs of the MnS thick film at different magnifications of 1000×, 3000×, 5000× and 10,000×, respectively.

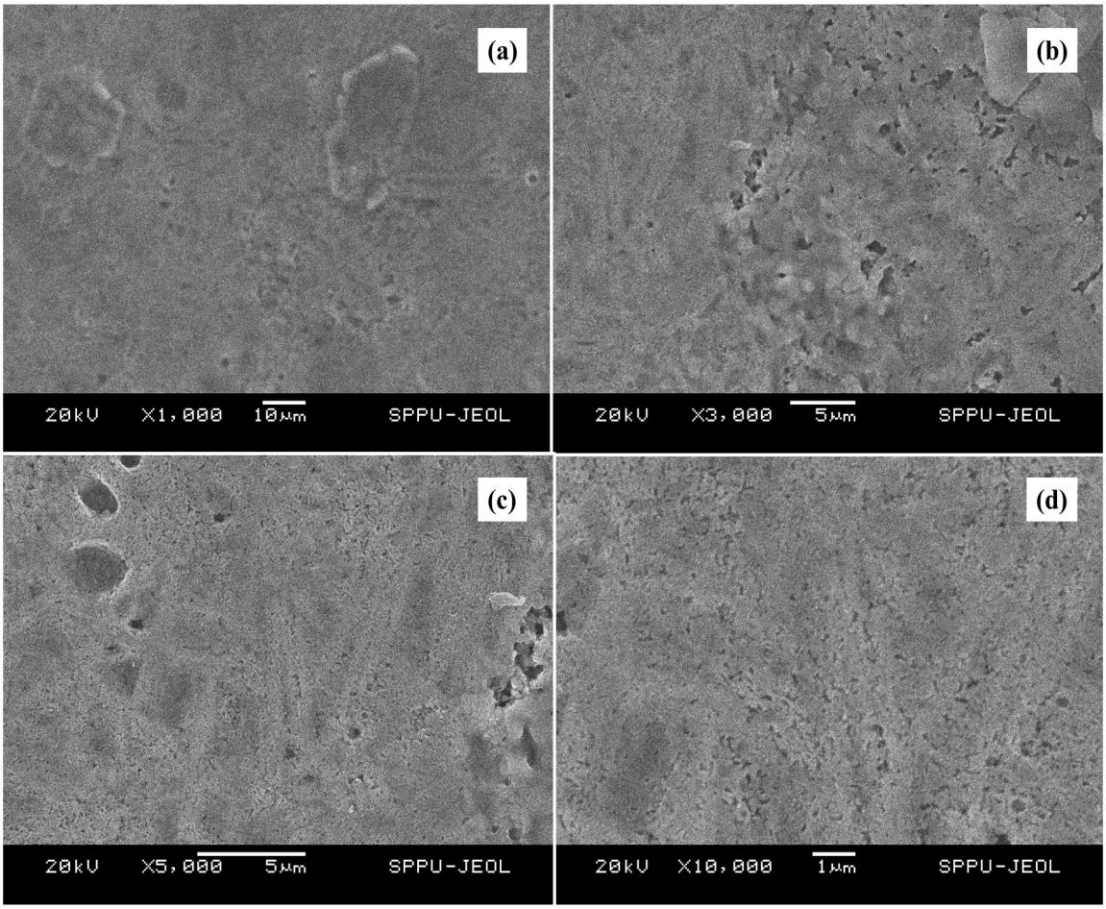

Figure 3 (a-d): SEM micrograph of MnS thick films at different magnifications

The SEM analysis provides detailed information regarding the surface morphology, particle distribution, agglomeration, surface uniformity and microstructural characteristics of the screen-printed MnS thick film. At 1000× magnification [Figure 3(a)], the MnS film exhibits a continuous surface with irregularly distributed morphological features and localized agglomerated regions. The surface appears relatively compact at this magnification, although variations in contrast indicate differences in particle packing and surface texture. Such morphological characteristics originate from the deposition of MnS nanopowder in the presence of organic binders during screen printing. Chaki et al. (2017) reported that MnS films deposited on glass

substrates exhibit a homogeneous surface consisting of spherical grains with different size distributions, demonstrating that the preparation conditions strongly influence the surface morphology of MnS films. At 3000× magnification [Figure 3(b)], the surface features become more distinguishable. The micrograph reveals fine particulate features distributed throughout the film together with localized clusters and small irregular depressions. The presence of these features indicates non-uniform packing of MnS nanopowder particles during formation of the thick-film layer. The 70:30 MnS-to-organic binder composition provides the paste with suitable printability, while drying and subsequent annealing modify the arrangement of the deposited particles. During thermal treatment at 200 °C for 2 h, the organic constituents undergo removal and the MnS particles establish stronger interparticle contact, producing a mechanically stable film. The morphology of MnS is strongly dependent on preparation parameters. Hannachi et al. (2017) demonstrated that changes in deposition conditions and thermal annealing produce substantial variations in MnS film morphology, including hexagonal, spherical, cubic and flower-like structures. The SEM image at 5000× magnification [Figure 3(c)] provides greater detail of the surface microstructure. Fine MnS particles are distributed over the film surface, accompanied by localized agglomerated regions and several irregular dark cavities. The dark regions represent surface depressions or void-like features associated with incomplete packing of particles during screen-printing deposition. The presence of these features is consistent with the particulate nature of the starting MnS nanopowder and the binder-assisted printing process. The morphology observed in the present film differs from the highly defined spherical or hexagonal morphologies reported for solution-grown MnS films because the present material originates from commercially available MnS nanopowder, which is directly formulated into a printable paste. Dhandayuthapani et al. (2015) reported that MnS films exhibit significant morphological changes with changes in precursor conditions, including spherical, almond-like and cauliflower-like structures, and related these variations to particle aggregation and film-growth conditions. At the highest magnification of 10,000× [Figure 3(d)], the MnS thick film displays a fine granular surface with closely distributed microstructural features. The surface appears comparatively homogeneous over the observed region, with small-scale irregularities and closely packed particles. The absence of large cracks across the examined area indicates good continuity of the deposited MnS layer. The fine surface texture is associated with the nanoscale nature of the starting MnS powder and its consolidation during thermal treatment. Lokhande et al. (1998) reported that MnS films deposited on glass substrates consist of nanocrystalline grains and demonstrated that the film-growth conditions influence grain structure and surface characteristics. The present SEM observations indicate that the screen-printing process produces a continuous MnS thick-film layer with localized particle agglomeration and surface cavities. The morphology observed at different magnifications also provides an important correlation with the XRD results. The XRD analysis gives information about the crystalline domains, whereas SEM reveals the physical arrangement of particles and grains over the film surface. The calculated crystallite size of 86 nm from XRD represents the coherently diffracting crystalline domains and does not directly represent the larger surface features observed in SEM. Several crystalline domains can exist within a single larger particle or agglomerated region, producing a difference between XRD crystallite size and SEM-observed morphological size. Chaki et al. (2017) similarly reported a polycrystalline MnS film in which XRD-derived crystallite dimensions differed substantially from the grain dimensions observed by SEM

3.3 energy-dispersive X-ray spectroscopy (EDX)

Figure 4 presents the EDX spectrum of the screen-printed MnS thick film, while Table 1 summarizes its elemental composition. The EDX spectrum exhibits distinct characteristic peaks corresponding to manganese (Mn) and sulfur (S), confirming the presence of the two principal constituent elements of the MnS film. The Mn signals observed in the low-energy region and around the higher-energy Mn characteristic lines originate from the interaction of the incident electron beam with Mn atoms, whereas the peak located near 2.3 keV

corresponds to the characteristic sulfur signal. No additional prominent elemental peaks associated with foreign impurities are evident in the spectrum, confirming the compositional purity of the analyzed MnS layer within the detection capability of the EDX technique.

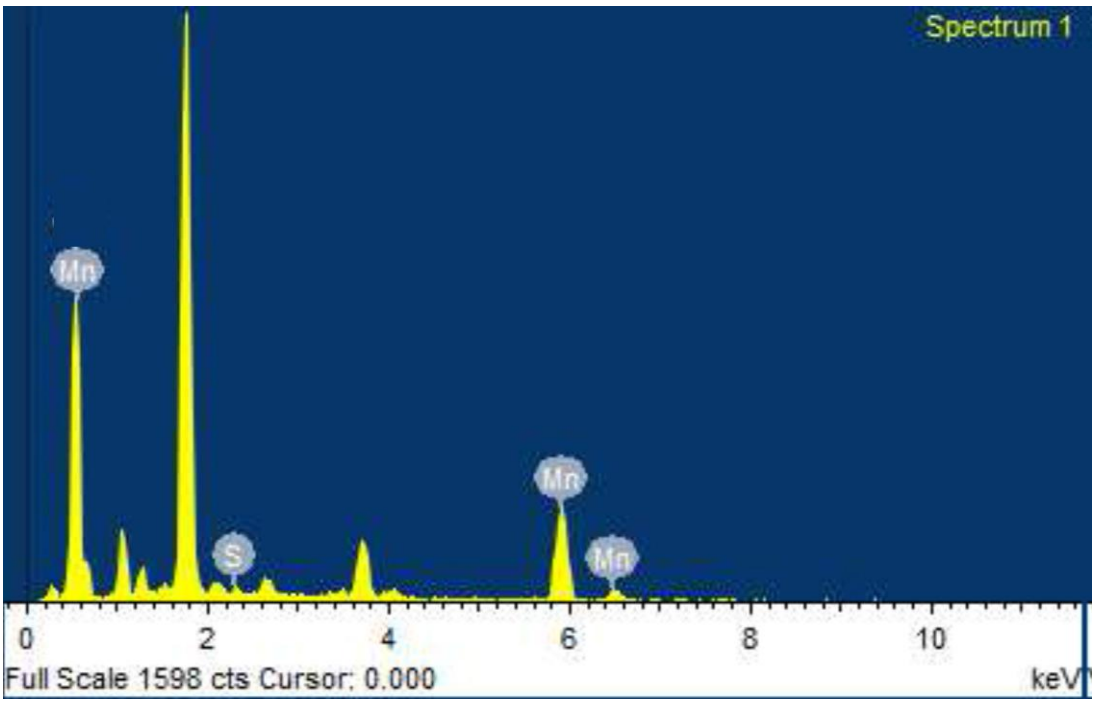

Figure 4: EDX spectra of MnS thick films

Table 1. EDX elemental composition of MnS thin film.

Element	Weight %	Atomic %
Mn	63.75	85.07
S	36.25	14.93
Total	100.00	100.00

Chaki et al. (2017) reported EDX analysis of MnS films prepared on glass substrates and observed characteristic Mn and S signals without detectable impurity elements, confirming the formation of MnS. The quantitative EDX analysis given in Table 1 shows 63.75 wt.% Mn and 36.25 wt.% S, giving a total elemental composition of 100 wt.%. These values are in close agreement with the theoretical elemental composition of stoichiometric MnS, which contains approximately 63.15 wt.% Mn and 36.85 wt.% S. Chaki et al. (2017) reported 64.77 wt.% Mn and 35.23 wt.% S for chemically deposited MnS films and compared these values with the theoretical MnS composition of 63.15 wt.% Mn and 36.85 wt.% S, demonstrating close agreement between experimental and theoretical weight percentages. The present values of 63.75 wt.% Mn and 36.25 wt.% S therefore show a close correspondence with the theoretical MnS composition, indicating that the fabricated thick film possesses an Mn-rich/S-containing composition close to the expected MnS stoichiometry. Chowdhury et al. (2011) also confirmed the presence of Mn and S in MnS films through EDX and reported an approximately stoichiometric MnS composition.

4. Conclusion

- MnS thick films were successfully fabricated on glass substrates using the screen-printing technique.
- XRD confirmed the hexagonal γ-MnS phase corresponding to JCPDS No. 40-1289.
- The average crystallite size was determined as 86 nm.

- SEM revealed a fine-grained, continuous surface with localized agglomeration and pores.
- EDX confirmed the presence of Mn and S, with 63.75 wt.% Mn and 36.25 wt.% S.
- The results confirm the successful formation of MnS thick films with well-defined structural, morphological and elemental characteristics.

Acknowledgment

The authors sincerely thank the Department of Physics and Research Centre, MGV's Arts, Science and Commerce College, Malegaon, Maharashtra, India, for providing the necessary laboratory facilities and support for carrying out the present research work. The authors also express their sincere gratitude to the Department of Physics, Savitribai Phule Pune University (SPPU), Pune, Maharashtra, India, for providing the necessary facilities for XRD, SEM and EDS/EDX characterization of the prepared MnS thick films.

REFERENCES:

1. Beltran-Huarac, J., Palomino, J., Resto, O., Wang, J., Jadwisienczak, W. M., Weiner, B. R., & Morell, G. (2014). Highly-crystalline γ-MnS nanosaws. RSC Advances, 4, 38103–38110.
2. Chaki, S. H., Chauhan, S. M., Tailor, J. P., & Deshpande, M. P. (2017). Synthesis of manganese sulfide (MnS) thin films by chemical bath deposition and their characterization. Journal of Materials Research and Technology, 6(2), 123–128.
3. Chowdhury, M. R. I., Podder, J., & Islam, A. B. M. O. (2011). Synthesis and characterization of manganese sulphide (MnS) thin films deposited by spray pyrolysis. Crystal Research and Technology, 46(3), 267–271.
4. Dhandayuthapani, T., Girish, M., Sivakumar, R., Sanjeeviraja, C., & Gopalakrishnan, R. (2015). Tuning the morphology of metastable MnS films by simple chemical bath deposition technique. Applied Surface Science, 353, 449–458.
5. Gao, Y., Feng, J., Liu, F., & Liu, Z. (2022). Effects of organic vehicle on the rheological and screen-printing characteristics of silver paste for LTCC thick film electrodes. Materials, 15(5), 1953.
6. Gümüş, C., Ulutaş, C., Esen, R., Özkendir, O. M., & Ufuktepe, Y. (2005). Preparation and characterization of crystalline MnS thin films by chemical bath deposition. Thin Solid Films, 492(1–2), 1–5.
7. Hannachi, A., & Maghraoui-Meherzi, H. (2017). Growth of different phases and morphological features of MnS thin films by chemical bath deposition: Effect of deposition parameters and annealing. Journal of Solid State Chemistry, 247, 120–130.
8. Inukai, K., Takahashi, Y., Ri, K., & Shin, W. (2015). Rheological analysis of ceramic pastes with ethyl cellulose for screen-printing. Ceramics International, 41(4), 5959–5966.
9. Lokhande, C. D., Ennaoui, A., Patil, P. S., Giersig, M., Muller, M., Diesner, K., & Tributsch, H. (1998). Process and characterisation of chemical bath deposited manganese sulphide (MnS) thin films. Thin Solid Films, 330(2), 70–75.
10. Pujari, R. B., Lokhande, A. C., Yadav, A. A., Kim, J. H., & Lokhande, C. D. (2016). Synthesis of MnS microfibers for high-performance flexible supercapacitors. Materials & Design, 108, 510–517.
11. Suryawanshi, P. S., Patil, A. V., Padhye, G. G., & Tupe, U. J. (2024). Investigation the influence of calcination temperature on structural, electrical and gas sensing properties MnO_2 thick films. Advanced Materials Research, 1180, 67–81.
12. Taşdemirci, T. Ç. (2025). Impact of annealing temperature on physical properties of manganese sulfide thin film. Kocaeli Journal of Science and Engineering, 8(1), 86–93.

13. Tupe, U. J., Zambare, M. S., Patil, A. V., & Koli, P. B. (2020). The binary oxide NiO–CuO nanocomposite based thick film sensor for the acute detection of hydrogen sulphide gas vapours. Materials Science Research India, 17(3), 260–269.
14. Tupe, U. J., Patil, A. V., Zambare, M. S., & Koli, P. B. (2021). Stannous oxide thick film nanosensors design by screen printing technology: Structural, electrical parameters and H_2S gas detection study. Materials Science Research India, 18(1), 66–74.
15. Wang, S., Li, K., Zhai, R., Wang, H., Hou, Y., & Yan, H. (2005). Synthesis of metastable γ-manganese sulfide crystallites by microwave irradiation. Materials Chemistry and Physics, 91, 298–300.
16. Zhao, P., Zeng, Q., He, X., Tang, H., & Huang, K. (2008). Preparation of γ-MnS hollow spheres consisting of cones by a hydrothermal method. Journal of Crystal Growth, 310, 4268–4272.